



저작자표시-비영리-변경금지 2.0 대한민국

이용자는 아래의 조건을 따르는 경우에 한하여 자유롭게

- 이 저작물을 복제, 배포, 전송, 전시, 공연 및 방송할 수 있습니다.

다음과 같은 조건을 따라야 합니다:



저작자표시. 귀하는 원저작자를 표시하여야 합니다.



비영리. 귀하는 이 저작물을 영리 목적으로 이용할 수 없습니다.



변경금지. 귀하는 이 저작물을 개작, 변형 또는 가공할 수 없습니다.

- 귀하는, 이 저작물의 재이용이나 배포의 경우, 이 저작물에 적용된 이용허락조건을 명확하게 나타내어야 합니다.
- 저작권자로부터 별도의 허가를 받으면 이러한 조건들은 적용되지 않습니다.

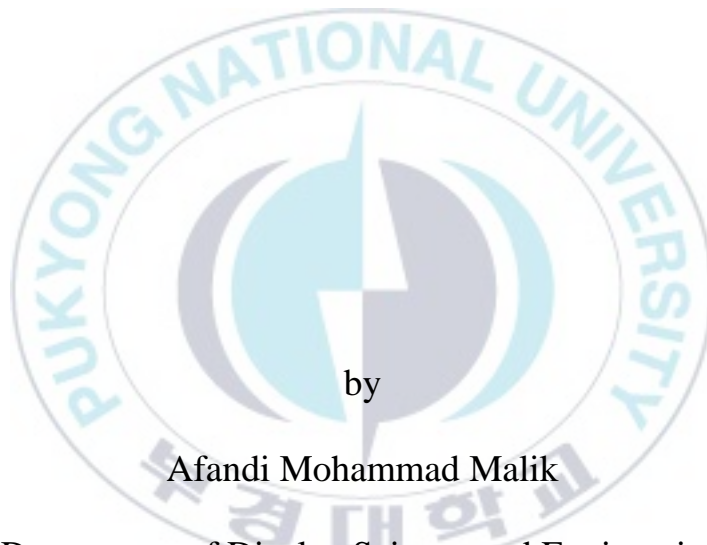
저작권법에 따른 이용자의 권리는 위의 내용에 의하여 영향을 받지 않습니다.

이것은 [이용허락규약\(Legal Code\)](#)을 이해하기 쉽게 요약한 것입니다.

[Disclaimer](#)

Thesis for the Degree of Master Engineering

Thin-Film Electroluminescent Device of  
 $\text{Y}_2\text{SiO}_5:\text{Eu}^{3+}$  Red Phosphor on Silicon  
Wafer



by

Afandi Mohammad Malik

Department of Display Science and Engineering

Graduate School of Engineering

Pukyong National University

August 24, 2018

Thin-Film Electroluminescent Device of  
 $Y_2SiO_5:Eu^{3+}$  Red Phosphor on Silicon  
Wafer

(실리콘 웨이퍼상의  $Y_2SiO_5:Eu^{3+}$  적색  
형광체의 박막 전계 발광 소자)

Advisor: Prof. Jongsu Kim

by

Afandi Mohammad Malik

A thesis submitted in partial fulfillment of the requirements  
for the degree of  
Master Engineering

in Department of Display Science and Engineering  
Graduate School of Engineering  
Pukyong National University

August 2018

Thin-Film Electroluminescent Device of  $Y_2SiO_5:Eu^{3+}$  Red  
Phosphor on Silicon Wafer

A dissertation  
by  
Afandi Mohammad Malik

Approved by:

\_\_\_\_\_  
(Chairman) Jong Tae Kim

\_\_\_\_\_  
(Member) Jong Su Kim

\_\_\_\_\_  
(Member) Yong Seok Jeong

August 24, 2018

# Contents

<b>Contents</b> .....	<b>i</b>
<b>List of Figures</b> .....	<b>iv</b>
<b>List of Tables</b> .....	<b>vi</b>
<b>Acknowledgements</b> .....	<b>vii</b>
<b>Abstract</b> .....	<b>ix</b>
<b>Chapter 1 Introduction</b> .....	<b>1</b>
<b>Chapter 2 Background</b> .....	<b>4</b>
1. Electroluminescence .....	4
1.1 Various Electroluminescent Devices .....	4
1.2 Alternating Current Thin Film Electroluminescent Device...	6
2. Sol-Gel Coating Method .....	10
2.1 Sol-Gel .....	10
2.2 Spin Coating.....	11
3. Oxide Phosphor for EL Devices .....	13
3.1 Various Types of Oxide Phosphor .....	13

3.2 Y <sub>2</sub> SiO <sub>5</sub> Host Lattice .....	14
3.3 Activators .....	15
3.4 Thermal Quenching Behavior.....	18
<b>Chapter 3 Experimental Procedures .....</b>	<b>19</b>
1. Sol-Gel Preparation.....	19
1.1 Y <sub>2</sub> SiO <sub>5</sub> Phosphor Solution.....	19
1.2 SiO <sub>2</sub> Dielectric Solution.....	21
2. Thin Film Electroluminescent Device .....	21
2.1 Silicon Wafer Substrate .....	21
2.2 Spin Coating of Y <sub>2</sub> SiO <sub>5</sub> :Eu <sup>3+</sup> Phosphor.....	22
2.3 Spin Coating of SiO <sub>2</sub> .....	23
2.4 Heat Treatment.....	24
2.5 Sputtering of ITO.....	24
3. Measurements .....	25
3.1 Morphological Measurements .....	25
3.2 PL and PLE Measurements.....	26
3.3 Opto-Electrical EL Measurements.....	26
<b>Chapter 4 Results and Discussion .....</b>	<b>28</b>

1. Structural Characteristics .....	28
1.1 FE-SEM Image of $Y_2SiO_5:Eu^{3+}$ Phosphor.....	28
1.2 XRD Pattern of $Y_2SiO_5:Eu^{3+}$ Phosphor .....	30
1.3 EDX Spectrum of $Y_2SiO_5:Eu^{3+}$ Phosphor .....	31
2. Optical Properties.....	32
2.1 PLE, PL and EL Spectra .....	32
2.2 Decay Curve.....	34
2.3 Time Chart .....	36
2.4 Reflectance.....	38
3. Opto-Electric Properties.....	39
3.1 Voltage-Dependent EL Spectra .....	39
3.2 Frequency-Dependent EL Spectra .....	43
3.3 Temperature-Dependent EL Spectra.....	45
4. Electrical Properties .....	49
4.1 Q-V Characteristics.....	49
4.2 Efficiency and Power Consumption .....	51
<b>Chapter 5 Conclusion.....</b>	<b>53</b>
<b>References.....</b>	<b>55</b>

## List of Figures

Figure 1. Classification of Electroluminescent Device .....	5
Figure 2. Cross-Sectional of ACTFEL Structure .....	8
Figure 3. ACTFEL Mechanism .....	9
Figure 4. Sol-Gel Process .....	11
Figure 5. Spin Coating Deposition Process .....	12
Figure 6. The General PL and PLE Spectrum of Eu Material.....	17
Figure 7. $\text{Y}_2\text{SiO}_5:\text{Eu}^{3+}$ sol-gel Phosphor Process .....	20
Figure 8. $\text{Y}_2\text{SiO}_5:\text{Eu}^{3+}$ ACTFEL Device Structure.....	23
Figure 9. Sawyer-Tower Circuit Preparation .....	27
Figure 10. FE-SEM Image of $\text{Y}_2\text{SiO}_5:\text{Eu}^{3+}$ ACTFEL Device.....	29
Figure 11. XRD Pattern of $\text{Y}_2\text{SiO}_5:\text{Eu}^{3+}$ Thin Film .....	30
Figure 12. EDX Scan of $\text{Y}_2\text{SiO}_5:\text{Eu}^{3+}$ Film.....	31
Figure 13. PLE, PL and EL Spectra of $\text{Y}_2\text{SiO}_5:\text{Eu}^{3+}$ ACTFEL Device..	33
Figure 14. PL Decay Time of $\text{Y}_2\text{SiO}_5:\text{Eu}^{3+}$ Phosphor.....	35
Figure 15. <i>V-I-EL</i> Time Chart of ACTFEL Device .....	37

Figure 16. Reflectance of $\text{Y}_2\text{SiO}_5:\text{Eu}^{3+}$ Thin Film on Si Wafer.....	38
Figure 17. EL Spectra of ACTFEL Device with the Various Applied Voltage at 400 Hz.....	40
Figure 18. Luminance-Voltage ( $L$ - $V$ ) Characteristics of Device.....	42
Figure 19. EL Spectra of ACTFEL Device with the Various Applied Frequencies at 80 V.....	43
Figure 20. Luminance-Frequency ( $L$ - $f$ ) Characteristics of Device.....	45
Figure 21. Luminance-Temperature ( $L$ - $T$ ) Characteristics of Device ....	47
Figure 22. EL Spectra of ACTFEL Device with the Various Temperature at 80 V and 400 Hz.....	48
Figure 23. Charge Density-Voltage ( $Q$ - $V$ ) Characteristics of Device ....	50
Figure 24. Efficiency, Luminance, and Power Consumption-Voltage ( $\eta, L$ , $P$ - $V$ ) Characteristics of ACTFEL Device.....	52

## List of Tables

Table 1	Electron Configuration of Rare-Earth Elements .....	16
Table 2	The EDX Contents of $Y_2SiO_5:Eu^{3+}$ Thin Film.....	32



## Acknowledgements

First of all, I would like to say thank for my God, Allah, which gave to me the precious live and healthy. The next are my mother, father and my brother who always cheer me up for everything in my live and supporting me in countlessly. I could not complete my thesis without their plentiful support and endless love.

I am heartily thankful to my supervisor, Prof. Jong Su Kim, not only for giving me an opportunity to go further distance, but for his invaluable guidance. Encouragement and inspiration in my academic work. His thoughtfulness deeply motivated me throughout this research process I acknowledge members of my thesis committee, Prof. Jong Tae Kim, and Prof. Yong Seok Jeong for their support, constructive criticism, and valuable input.

I take this opportunity to thank all the professors in the Department of Display Science and Engineering, Pukyong National University, for their support and encouragement. For financial support, I would like to express my sincere gratitude to Pukyong National University and Brain Korea (BK21)

program for providing me the scholarship support for my study in Korea. This research would have not been possible without the financial support from these organizations.

I also thank my lab-mates in Inorganic Emitting Laboratory including Taewook Kang, Daehan Kim, Wunho Lee, Jongho Ryu, Jaehyeong Kim, Byungjoo Jeon, Hyojun Kim, Soonho Lee, Yeongwoo Jeong, and all of the friends at the Department of Display Science and Engineering for creating a pleasant working atmosphere. I feel thankful to Dr. Taehun Kim and the senior in our laboratory including Dr. Sunghun Lee and Dr. Jehong Park for their continuous support technically and mentally.

Lastly, I offer my regards and blessings to all of those who supported me in any respect during the completion of the thesis and the study,

# Thin-Film Electroluminescent Device of $\text{Y}_2\text{SiO}_5:\text{Eu}^{3+}$ Red Phosphor on Silicon Wafer

Afandi Mohammad Malik

Department of Display Science and Engineering  
Graduate School of Engineering  
Pukyong National University

## Abstract

The red alternating current thin film electroluminescent (ACTFEL) device has been demonstrated by using  $\text{Eu}^{3+}$ -activated  $\text{Y}_2\text{SiO}_5$  phosphor as an emitting layer. The ACTFEL device consists of indium tin oxide (ITO) top electrode, sandwiched  $\text{SiO}_2$  dielectric layer and  $\text{Y}_2\text{SiO}_5:\text{Eu}^{3+}$  layer grown on N-type Si wafer as bottom electrode. The phosphor layer is prepared through a sol-gel based spin coating method, which was annealed at  $1200^\circ\text{C}$  for 4 hours in air atmosphere. The PLE spectrum has 250 nm peak which result from charge transfer state (CTS) transition. The PL spectrum has 585 and 610 nm main peaks, which are attributed to  $^5\text{D}_0 \rightarrow ^7\text{F}_1$  and  $^5\text{D}_0 \rightarrow ^7\text{F}_2$  transition of  $\text{Eu}^{3+}$  in  $\text{Y}_2\text{SiO}_5:\text{Eu}^{3+}$  phosphor, respectively. The EL device emits the sharp red spectrum with a luminance of  $1.6 \text{ cd/m}^2$  at 80 V and 400 Hz while the highest efficiency is  $0.6 \text{ lm/W}$  at 45 V with the same frequency. The EL device shows the exponential increase to AC voltage and the linear increase to frequency with a threshold voltage ( $V_{\text{th}}$ ) of 40 V. The luminance is relatively stable with the increasing of temperature in the range of  $20\text{-}80^\circ\text{C}$ . However, the luminance is decreased gradually after

80°C due to thermal quenching effect of the phosphor. Finally, this EL device exhibits stable constant color in the extreme hot condition without changing its spectra.

Key Words: Thin Film Electroluminescent Device,  $\text{Y}_2\text{SiO}_5:\text{Eu}^{3+}$ , Silicon wafer, Red emission



## 실리콘 웨이퍼상의 $Y_2SiO_5:Eu^{3+}$ 적색 형광체의 박막 전계 발광 소자

Afandi Mohammad Malik

융합디스플레이공학과

공과대학

국립부경대학교

### 요약

적색 교류 박막 전계 발광 (ACTFEL) 소자는  $Eu^{3+}$  활성화  $Y_2SiO_5$  형광체를 발광층으로 사용하여 제작되었다. ACTFEL 소자는 인듐 주석 산화물 (ITO) 상부 전극, 샌드위치 구조인  $SiO_2$  유전체층 및 하부 전극으로서 N type Si 웨이퍼 상에 제작된  $Y_2SiO_5:Eu^{3+}$  층으로 구성된다. 형광체층은 졸-겔 기반 스핀 코팅 방법을 통해 제조되었고, 공기 분위기에서  $1200\text{ }^\circ\text{C}$  에서 4 시간 동안 열처리하였다. PLE 스펙트럼은 전하 이동 상태 (CTS) 전이로부터 기인한  $250\text{ nm}$  피크를 갖는다. PL 스펙트럼은  $Y_2SiO_5:Eu^{3+}$  형광체에서 각각  $5D^0 \rightarrow 7F^1$  및  $5D^0 \rightarrow 7F^2$  전이에 해당하는  $585$  및  $610\text{ nm}$  주 피크 스펙트럼을 갖는다. EL 소자는 넓은 적색 스펙트럼을 방출하고  $80\text{ V}$  및  $400\text{ Hz}$  에서  $1.6\text{ cd/m}^2$ 의 휘도를 가지지만 효율은  $45\text{ V}$ 에서 최고  $0.6\text{ lm/W}$ 이다. EL 소자는 임계 전압 ( $V_{th}$ ) 이  $40\text{ V}$  이고, 전압에 따라 기하급수적으로 증가하고 주파수에 따라 선형적으로 증가하는 것을 보인다. 휘도는  $20\text{-}80\text{ }^\circ\text{C}$ 의 범위에서 상대적으로 안정했다. 그러나, 형광체의 열적 소광 효과로 인해  $80\text{ }^\circ\text{C}$  이후 점진적으로

감소한다. 마지막으로, 이 EL 소자는 스펙트럼을 변화시키지 않으면서 일정한 색을 나타내고, 고온에서 안정하다.

키워드: 박막 전계 발광 소자,  $Y_2SiO_5:Eu^{3+}$ , 실리콘 웨이퍼, 적색 방출



# Chapter I

## Introduction

The conventional thin film electroluminescent (EL) device for flat panel display provide by rare earth metal activated on sulfide phosphors such as ZnS, SrS, and CaS. These phosphors exhibit excellent EL properties including high brightness with relatively low threshold voltages. However, there are several intrinsic problems such as their chemical instability and the influence of moisture, make it difficult to pattern this phosphors by chemical etching or photolithography. There are rapid development to search for oxide phosphors with high electroluminescence efficiency, intrinsic chemical stability, and moisture resistance. The high optical transmissivity in the visible wavelength region also makes the oxide phosphors good candidate for multilayer and multicolor displays. Furthermore, the oxide phosphor also has high possibility to utilize the UV range spectrum as the surface emitting device. The most promising candidates are  $Zn_2SiO_4$  doped by Mn which has 525 nm green spectrum and  $Y_2SiO_5$  activated by Ce with 420 nm blue

spectrum. Some investigation reported that  $\text{Zn}_2\text{SiO}_4:\text{Mn}$  has the highest EL brightness up to  $3400 \text{ cd/m}^2$  at 5 kHz [1-3].

Oxide phosphors have recently attracted much attention for electroluminescent displays (ELD), field emission displays (FED) and plasma display panels (PDP) because of the variety of materials available and the higher chemical stability of oxide phosphors compared with sulfide phosphors [4]. In this study we will focus on the yttrium based of oxide phosphor. Yttrium silicate ( $\text{Y}_2\text{SiO}_5$ ) is a well-known luminescent host material for various rare-earth activators. It has high chemical stability which makes it a promising candidate for integrated planar displays which very important in thin film luminescent formation application [5].

Ouyang et al introduced the preparation and electroluminescence of the  $\text{Ce}:\text{Y}_2\text{SiO}_5$  thin film by RF magnetron sputtering and used it in a multilayer display [6]. On the other hand, this research will use metal-organic decomposition (MOD) as coating method. The MOD is a solution deposition method from sol-gel phase of mixing several materials before synthesis it on solid state reaction. Compare to sputtering method, MOD has the advantages such as simple process, low cost, easily adjusted composition and easily

activators changing. This process is suitable with optical integrated circuits, and it is easy to adapt to the realization of planar displays [7].

This study presents the effect of  $\text{Eu}^{3+}$  activator on the luminescence properties of both photoluminescence and electroluminescence of the thin film EL device. Moreover, this study will show the electrical behaviors of yttrium based oxide phosphor thin film such as voltage and frequency responses and charge density-voltage ( $Q$ - $V$ ) curve. Finally, for the feasibility test of the device, the temperature effect on EL performance will be measured and it shows a stable luminescence until it reaches a critical temperature, that is, the thermal quenching temperature.

# Chapter 2

## Background

### 1. Electroluminescence

#### 1.1 Various Electroluminescent Devices

The electroluminescence (EL) is a phenomenon of light which emitted when the electric field is applied to crystalline materials, or resulting from a current flow through an emissive semiconducting material such as phosphor. The inorganic materials based on EL classified by two groups: injection EL and high electric field EL. Injection EL is a radiation resulting from recombination of minority charge carriers injected to a p-n or pin junction, this junction is generally forward biased as in organic EL and LED. On the other hand, the high field EL is optical phenomenon and electrical phenomenon in which a material emits light in response to the passage of an electric current or to a strong electric field. High field EL divided into two types: powder based EL and also thin film EL. The classification of EL summarize in figure 1 [8-10].

The first EL was observed in 1936 by Destriau. The observed EL was from ZnS powder phosphor suspended in Castrol oil under strong electric field [11]. This type of EL is classified as powder based EL. In the early 1960s, polycrystalline ZnS thin film were used as EL materials and first thin film EL device was made [12]. Furthermore, in 1952, infrared EL from forward biased p-n junctions in Ge and Si diodes was reported and classified as injection type EL this is well-known LEDs [13].

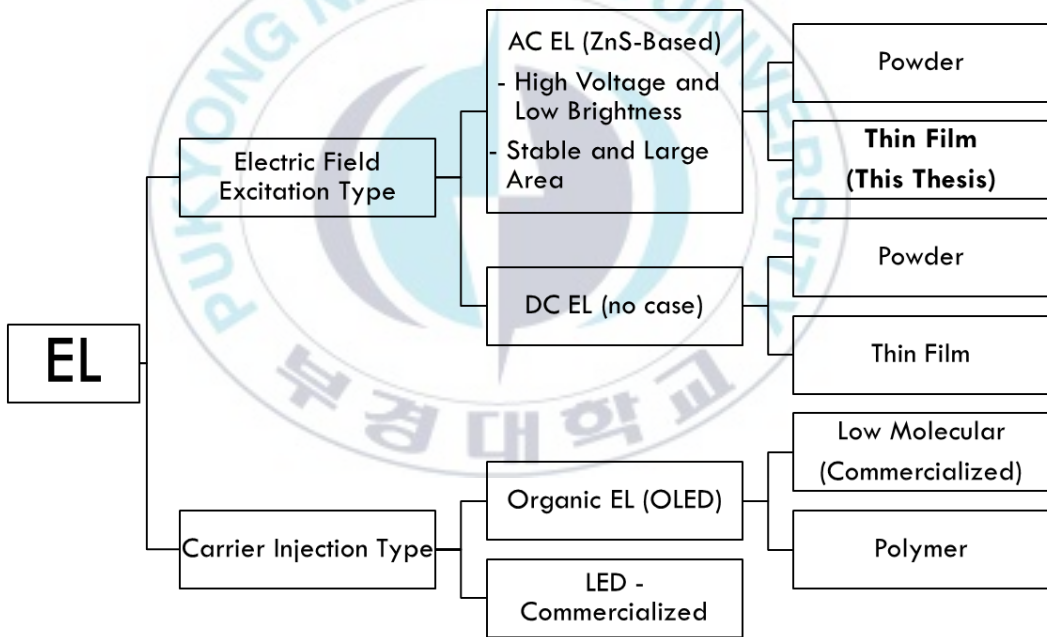


Figure 1. Classification of Electroluminescent Device

Visible EL is observed in diodes made using wide band gap semiconductors such as GaN. These diodes are called light emitting diodes (LED) and have been widely used since 1960s [14]. The mechanism of light generation by high field EL or injection type EL was quite different. The high field EL emits light when the high electric field is being applied to the emissive layer which has around 200-300 V, while the injection EL using carrier recombination phenomena to emits the light under lower voltage than the high field EL [15]. In this work, we will focus on the high field EL especially the alternating current thin film EL (ACTFEL) device.

## **1.2 Alternating Current Thin Film Electroluminescent (ACTFEL) Device**

The ACTFEL device operates by applying a large ( $\sim 100$  V) AC voltage across the external electrodes. An addressing scheme sequentially scans the row of the display while a modulating voltage is applied to the columns. Below the threshold voltage the structures behaves as a capacitor due to high resistivity of phosphor layer and charges flow primarily as reactive displacement current [16]. Figure 2 depicts the cross-sectional view of the typical of ACTFEL structures [17]. Basically ACTFEL device consists of emissive layer and dielectric layer which prevent the leakage current from applied voltage. There

are two classified structures of ACTFEL device, the first one is single insulating layer and double insulating layer which known as sandwich structure.

The main purpose of the insulating layer is to confine current across the phosphor layer and preventing breakdown. At the same time, the insulating layer creates high density of electron traps, thus acting as a source of hot carriers at high external voltages which can be seen on figure 3 [18-19]. In figure 3, the energy band gap of dielectric layer is 8.6 eV while the energy band gap of phosphor layer is 4.82 eV. The total thickness of this device is 2  $\mu\text{m}$  which makes the electric field across the structure is  $2.0 \times 10^7$  V/cm.

The double insulating layer, sandwich structure, has advantage at higher breakdown voltage compared with single insulating layer. However, those structures require higher voltage in the threshold state of the device.

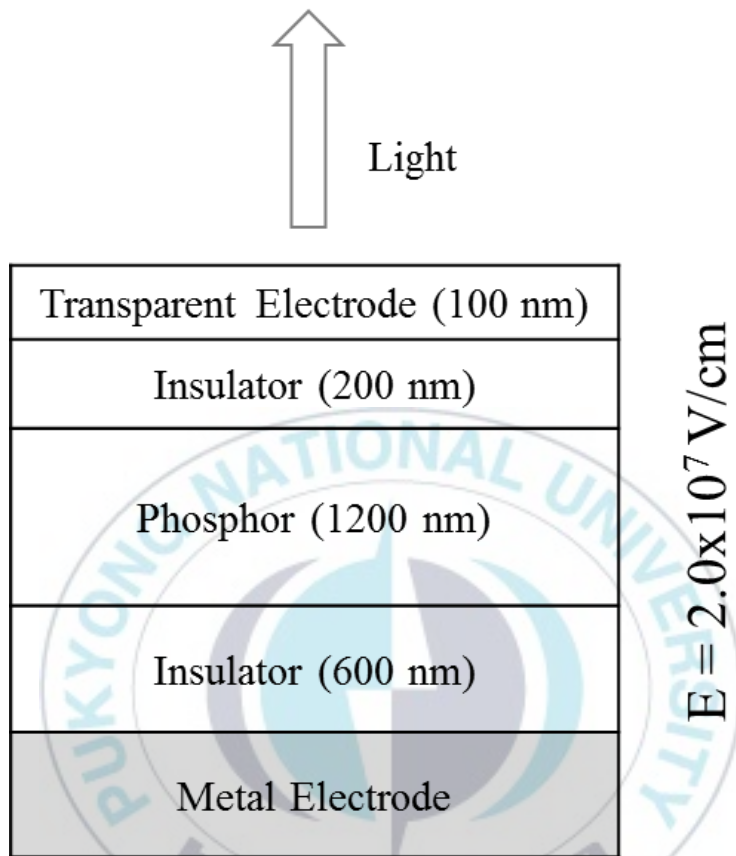


Figure 2. Cross-sectional of ACTFEL Structure



## 2. Sol-Gel Spin Coating Method

### 2.1 Sol-Gel

Sol-gel method is one of the well-established synthetic approaches to prepare novel metal oxide as well as mixed oxide. This method also well known as metal organic decomposition (MOD) which formed sol-gel phase of mixing several materials [7]. Sol-gel method mainly undergoes in few steps to deliver the final metal oxide protocols and those are hydrolysis, condensation, and drying process. This method has potential control over the textural and surface properties of the materials composites. The formation of metal oxide involves different consecutive steps, initially the corresponding metal precursor undergoes rapid hydrolysis to produce the metal hydroxide solution, followed by immediate condensation which leads to the formation of three-dimensional gels and ready to be the final product either Xerogel or Aerogel depending on the mode of drying which can be seen on figure 4. Sol-gel method can be classified into two kinds, such as aqueous sol-gel and nonaqueous sol-gel method depending on the nature of the solvent utilized [20-21].

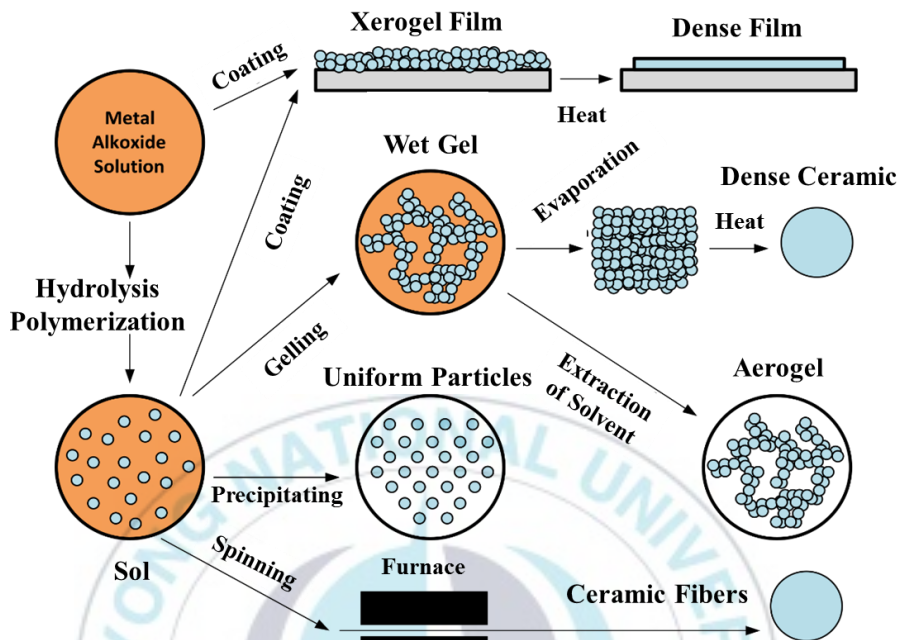


Figure 4. Sol-Gel Process

## 2.2 Spin Coating

Spin coating is one of the procedures which can be used to deposit a uniform thin film on a flat surface. Spin coating utilizes centrifugal force created by the spinning substrate to spread the deposition solution evenly over a surface. Spin coating can work with many types of coating solutions. If a liquid solution is placed in the center of the sample, and the sample spins at a given speed and time, the centrifugal forces will cause the liquid to spread evenly across the

sample. This process can be used effectively to control the amount of coverage of the actual coating solution by controlling the rotation speed and deposition time [22].

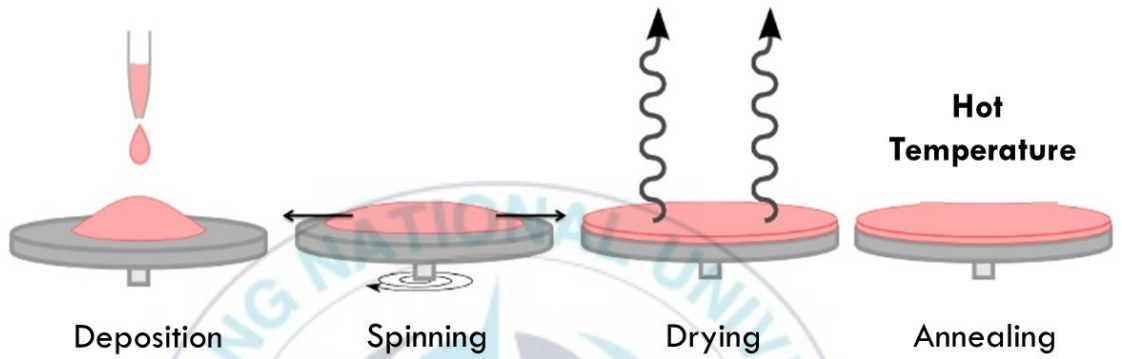


Figure 5. Spin Coating Deposition Process

### 3. Oxide Phosphors for EL Devices

#### 3.1 Various types of Oxide Phosphors

Oxide phosphors are widely used since 1990s. Minami et al reported that  $\text{Zn}_2\text{SiO}_4\text{:Mn}$  phosphor which deposited between  $\text{BaTiO}_3$  and conducting electrode emitted bright EL with efficiency up to 0.78 lm/W [23]. Oxide phosphors have recently attracted much attention for electroluminescent displays (ELD), field emission displays (FED) and plasma display panels (PDP) because of the variety of materials available and the higher chemical stability of oxide phosphors compared with sulfide phosphors [4].

The most well-known oxide phosphors are  $\text{Zn}_2\text{SiO}_4$ ,  $\text{ZnGa}_2\text{O}_4$  and  $\text{Y}_2\text{SiO}_5$ . In this study, we will focus on  $\text{Y}_2\text{SiO}_5$  phosphor as the host material with  $\text{Eu}^{3+}$ -activated materials. This phosphor has broad emission spectra from UVC range to the infra-red emission range with various doping. Therefore, this type of phosphor is suitable to be implicated in various EL based displays.

### 3.2 Y<sub>2</sub>SiO<sub>5</sub> Host Lattice

The role of host lattice determines the efficiency, chromaticity and brightness of the phosphor through interaction with the activator, creating a space that accepts the activator ion. Y<sub>2</sub>SiO<sub>5</sub> is well known wide band gap semiconductor that had been considered as an ideal host lattice for RE<sup>3+</sup> cations [24]. The band gap requires a similar energy gap to the visible light and should be a stable material that does not cause any chemical change during the process of electron beam irradiation

If there is a chemical bond that oscillates at a high frequency in a crystal, there is no chemical bond such as C-H or O-H because energy to be emitted is converted into vibration energy. As a condition for selecting the host, the size and the valence state should be similar to each other because the cation of the active agent substitutes for the cation site of the host. If the valence state is not similar, the luminescence characteristics will be significantly lowered due to the energy resonance phenomenon. In addition, when the arrangement of the activator electrons different from that of the parent cations, it is necessary to add the ions as a sensitizer to compensate the charge [25].

### 3.3 Activators

Since the active agent must be able to substitute within the atom of the host lattice, the charge must be balanced, and the atomic radius must be similar also so that the reaction is successful. According to the Hume-Rothery Rules, the ionic radius of the active agent should not exceed about 15% of the ionic radius of the host, the electronegativity should be similar, and the electrons should be similar. Finally, there is a condition that crystal structures must be equal to each other. Elements that comply with the above rule are universally suitable for Rare earth elements and these elements exhibit excellent color purity due to the internal transition of the vacant 4f electrons [25].

Table 1 depicts the RE cations configuration. In this study we are focusing on the Europium activator material as the dopant of  $Y_2SiO_5$  host lattice phosphor. Figure 6 shows the general luminescence properties of Europium material. Europium has broad 250 nm excitation while it has sharp 610 nm emission spectrum [26].

Table 1. Electron Configuration of Rare-Earth Elements

No	Element (Symbol)	Configuration	Ln <sup>3+</sup> Ion
1	Lanthanum (La)	[Xe] 5d6s <sup>2</sup>	[Xe] ([Kr]4d <sup>10</sup> 5s <sup>2</sup> 5p <sup>6</sup> )
2	Cerium (Ce)	[Xe] 4f <sup>5</sup> d6s <sup>2</sup>	[Xe] 4f
3	Praseodymium (Pr)	[Xe] 4f <sup>3</sup> 6s <sup>2</sup>	[Xe] 4f2
4	Neodymium (Nd)	[Xe] 4f <sup>4</sup> 6s <sup>2</sup>	[Xe] 4f3
5	Promethium (Pm)	[Xe] 4f <sup>5</sup> 6s <sup>2</sup>	[Xe] 4f4
6	Samarium (Sm)	[Xe] 4f <sup>6</sup> 6s <sup>2</sup>	[Xe] 4f5
7	Europium (Eu)	[Xe] 4f <sup>7</sup> 6s <sup>2</sup>	[Xe] 4f6
8	Gadolinium (Gd)	[Xe] 4f <sup>7</sup> 5d6s <sup>2</sup>	[Xe] 4f7
9	Terbium (Tb)	[Xe] 4f <sup>9</sup> 6s <sup>2</sup>	[Xe] 4f8
10	Dysprosium (Dy)	[Xe] 4f <sup>10</sup> 6s <sup>2</sup>	[Xe] 4f9
11	Holmium (Ho)	[Xe] 4f <sup>11</sup> 6s <sup>2</sup>	[Xe] 4f10
12	Erbium (Er)	[Xe] 4f <sup>12</sup> 6s <sup>2</sup>	[Xe] 4f11
13	Thulium (Tm)	[Xe] 4f <sup>13</sup> 6s <sup>2</sup>	[Xe] 4f12
14	Ytterbium (Yb)	[Xe] 4f <sup>14</sup> 6s <sup>2</sup>	[Xe] 4f13
15	Lutetium (Lu)	[Xe] 4f <sup>14</sup> 5d6s <sup>2</sup>	[Xe] 4f14

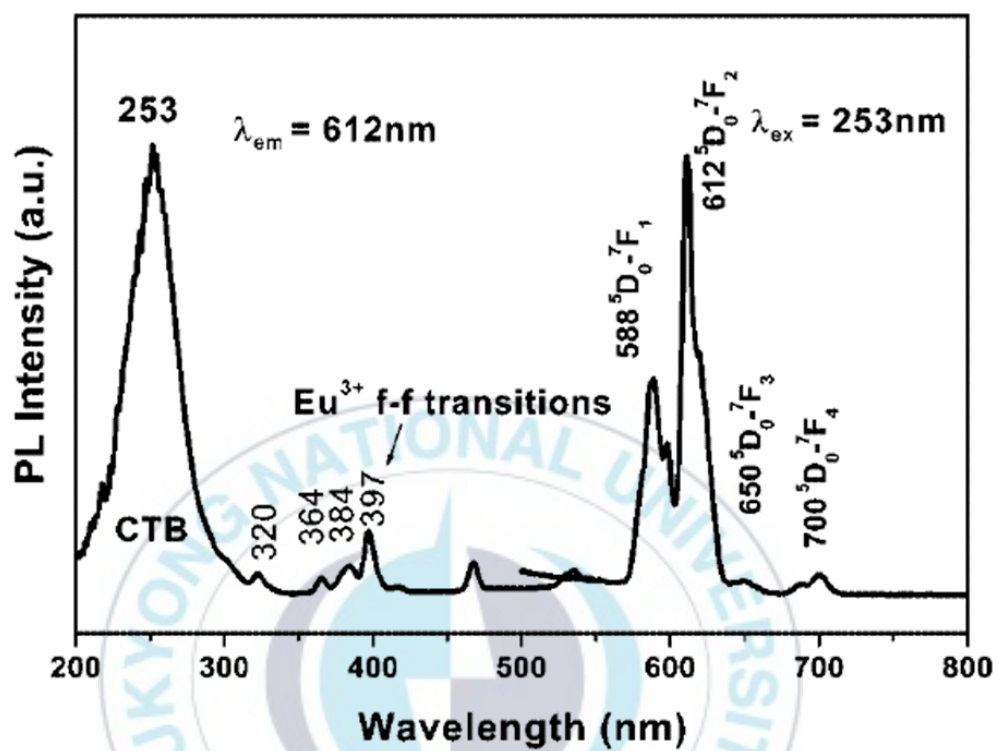


Figure 6. The General PL and PLE Spectra of Europium-doped phosphor

### 3.4 Thermal Quenching Behavior

Thermal quenching phenomenon occurs when the temperature of the phosphor increases; the brightness of light emission of the phosphor is lowered, and the wavelength band of light emission is red-shifted. As the temperature of the phosphor increases, the electrons that take thermal energy become more active and the number of excited electrons increases. Generally, the more electrons are excited, the more electrons are emitted and transited. However, the excitation and emission of electrons by heat energy are not selective excitation and emission of a specific range. As a result, when this phenomenon occurs, the emission wavelength becomes wider. In this way, the electrons obtaining heat energy are excited at a very stable level and excited at a higher energy level. After the phase is stabilized, stabilization is achieved in a relatively large area, not only at the lowest level. Temperature influences not only the emission wavelength range but also the energy band [27], the electrons reaching the contact point are not accompanied by light and fall to the low-energy band. This is a cause of lowering luminous efficiency. As a result, as the temperature of the mold increases, the emission wavelength band widens and the luminance decreases [28].

# Chapter 3

## Experimental Procedures

### 1. Sol-Gel Preparation

#### 1.1 $\text{Y}_2\text{SiO}_5:\text{Eu}^{3+}$ Phosphor Solution

Precursors of the  $\text{Eu}^{3+}$ -activated  $\text{Y}_2\text{SiO}_5$  were synthesized by the metal organic decomposition (MOD) technique. The starting materials are yttrium (III) nitrate hexahydrate ( $\text{Y}(\text{NO}_3)_3 \cdot 6\text{H}_2\text{O}$ , Sigma Aldrich, High Purity), tetra ethyl orthosilicate (TEOS,  $\text{Si}(\text{OC}_2\text{H}_5)_4$ , Kojundo Korea, Ultra High Purity). Rare-earth activator  $\text{Eu}^{3+}$  is obtained from europium (III) nitrate pentahydrate ( $\text{Eu}(\text{NO}_3)_3 \cdot 5\text{H}_2\text{O}$ , Sigma Aldrich, High Purity). The materials are mixed in acetic acid and 2-methoxy ethanol solvent in the magnetic stirrer in  $60^\circ\text{C}$  temperature for two hours to produce well solution of  $\text{Y}_2\text{SiO}_5:\text{Eu}^{3+}$ . Figure 7 depicts the sol-gel preparation process of  $\text{Y}_2\text{SiO}_5:\text{Eu}^{3+}$  phosphor.



Yttrium (III) nitrate hexahydrate  
( $\text{Y}(\text{NO}_3)_3 \cdot 6\text{H}_2\text{O}$ )



Europium (III) nitrate pentahydrate  
( $\text{Eu}(\text{NO}_3)_3 \cdot 5\text{H}_2\text{O}$ )

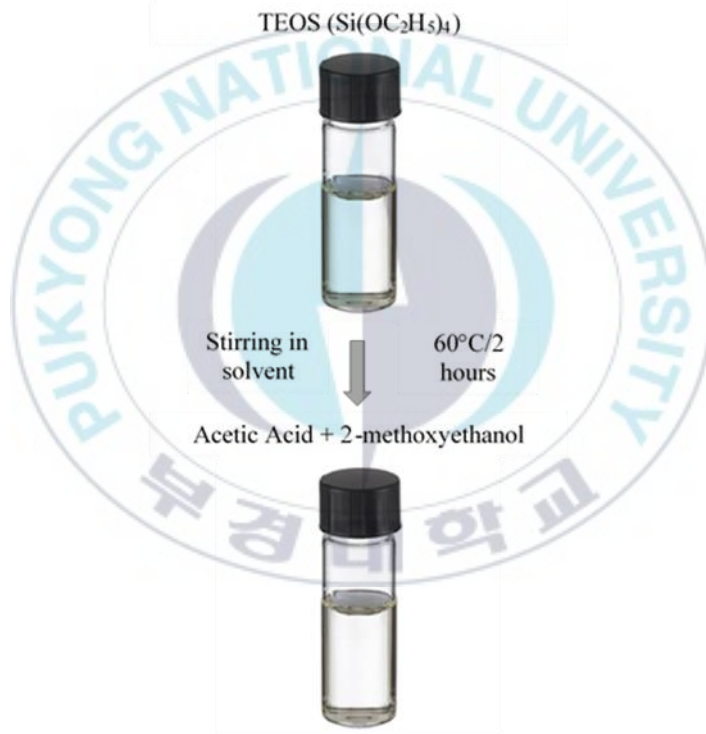


Figure 7.  $\text{Y}_2\text{SiO}_5:\text{Eu}^{3+}$  sol-gel Phosphor Process

## **1.2 SiO<sub>2</sub> Dielectric Solution**

The SiO<sub>2</sub> solution was obtained by mixing the TEOS (Si(OC<sub>2</sub>H<sub>5</sub>)<sub>4</sub>, Kojundo Korea, Ultra High Purity) with ethanol, distilled water and chloric acid (HCl) in room temperature for 16 hours. The ratio between Si and the solvent is 1:10 in order to make a well solution with good dielectric property. The solution was then spin coated in 2000 rpm for 30s and dry in 80°C for 15 minutes. The SiO<sub>2</sub> film obtained after it heat treatments in 500°C for two hours in air atmosphere.

## **2. Thin Film Electroluminescent Device**

### **2.1 Silicon Wafer Substrate**

A thin slice of n-type Si wafer material from Sehyoung Wafertech was used for substrate as well as bottom electrode. The n-type Si wafer have 82 Ω/sq sheet resistance and 400 μm thickness. In order to make a well deposit film on it, the n-type Si wafer was prepared by cleaning in four processes. Sonication cleaning process during 10 minutes each was accomplished in acetone, in ethanol and in isopropyl alcohol (IPA) respectively. Then ozone treatment for 10 minutes is followed to make its surface more hydrophilic.

## 2.2 Spin Coating of $\text{Y}_2\text{SiO}_5:\text{Eu}^{3+}$ Phosphor

The structure of this ACTFEL device can be seen on figure 8. This device using double insulating layer which sandwiched the emissive/phosphor layer in the middle. Therefore, before coating the phosphor, the  $\text{SiO}_2$  deposit on the Si wafer substrate first. After that the phosphor solution was spin coated on top of  $\text{SiO}_2$  layer in 2000 rpm for 30 seconds. The spin coated phosphor was then evaporated on hot plate at  $300^\circ\text{C}$  temperature for 10 minutes to remove the residual solvent. This process was repeated several times until the desired thickness was obtained. The thinner thickness of phosphor, the lower of its PL intensity, meanwhile too much phosphor also may result in poor thermal diffusion effect.

### 2.3 Spin Coating of SiO<sub>2</sub>

The solution of SiO<sub>2</sub> was spin coating in the Si wafer substrate in 2000 rpm for 30s and dry at 80°C for 15 minutes. The SiO<sub>2</sub> first film obtained after its heat treatment at 500°C for two hours in air atmosphere. After the phosphor deposited on top of the first SiO<sub>2</sub>, the sample then coats again with the second SiO<sub>2</sub> layer with the same condition. The last, the SiO<sub>2</sub> dielectric will sandwiched the phosphor in order to make better stability compare to only one dielectric layer.

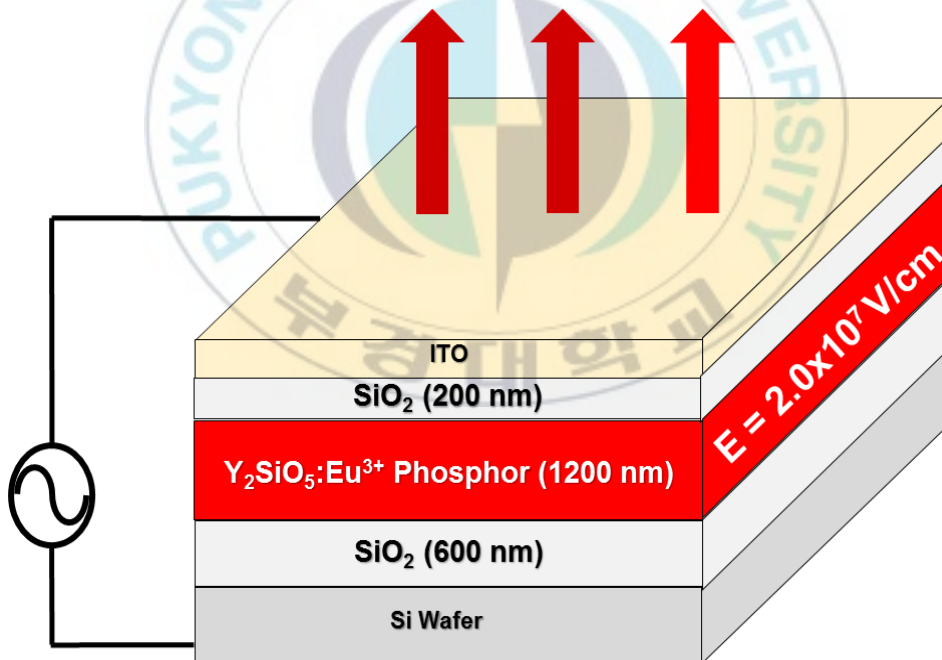


Figure 8. Y<sub>2</sub>SiO<sub>5</sub>:Eu<sup>3+</sup> ACTFEL Device Structure

## 2.4 Heat Treatment

The  $\text{Eu}^{3+}$ -activated  $\text{Y}_2\text{SiO}_5$  phosphor was synthesized by solid-state reactions method. Solid state reactions are performed in the absence of solvents by either grinding or melting the starting materials together or simply applying heat to a mixture of starting materials. The solid state reaction of the phosphor was occur in high temperature  $1200^\circ\text{C}$  for 4 hours to obtain the flat phosphor film. Solid state reactions offer reduced costs, decreased amounts of chemical waste and, sometimes, an increase in yield.

## 2.5 Sputtering of ITO

ITO is the most common transparent electrode which has been used widely for electroluminescent display. ITO has over 95% transmittance in visible range area with high conductivity and low resistance [29]. Therefore, at our ACTFEL device, ITO as its transparent top electrode is sputtered by a radio frequency (RF) magnetron sputtering (Vacuum Science VSMS-23A) with 90% transmittance and  $62 \Omega/\text{sq}$  sheet resistance.

### 3. Measurements

#### 3.1 Morphological Measurement

In this work, the experimental samples were sintered in furnace at 1200°C for 4 hours with 10°C/min heat rate in air atmosphere. The final product of this reaction is cleaned, flat and uniform surface of deposited phosphor. To observe the morphology and thickness of phosphor layer, field emission-scanning electron microscope (FE-SEM, Tescan VEGA II LSU) was used to capture the image both on surface or cross-sectional image. To identify the crystal structure of the phosphor, X-ray diffraction (XRD) pattern was measured from  $2\theta = 10^\circ$  to  $60^\circ$  using an X-ray diffractometer (Rigaku, Ultima IV). The reflectance was measured using Konica Minolta CM-3600d spectrometer.

### **3.2 PL and PLE Measurement**

PL is a light emission from any form of matter after the absorption of photons (electromagnetic radiation) [32]. The PL and PLE spectrum was measured by fluorescence spectrometer (Hitachi, F-4500) under room temperature and low level humidity (30%).

### **3.3 Opto-Electrical EL Measurements**

The ACTFEL device was connected to variable power supply with voltage variables from 0-100 V and 50-1000 Hz frequencies (Sinson Electronics). The EL spectrum was measure by Konica Minolta CS-2000 with the fixed distance (70 cm) and low level of humidity (30%). On the other hand, the charge density versus voltage (Q-V) characteristics was measured by Sawyer-Tower circuit using 0.47  $\mu$ F sense capacitor which can be seen on figure 9 and the data was recorded by digital oscilloscope (Textronix TDS2012B).

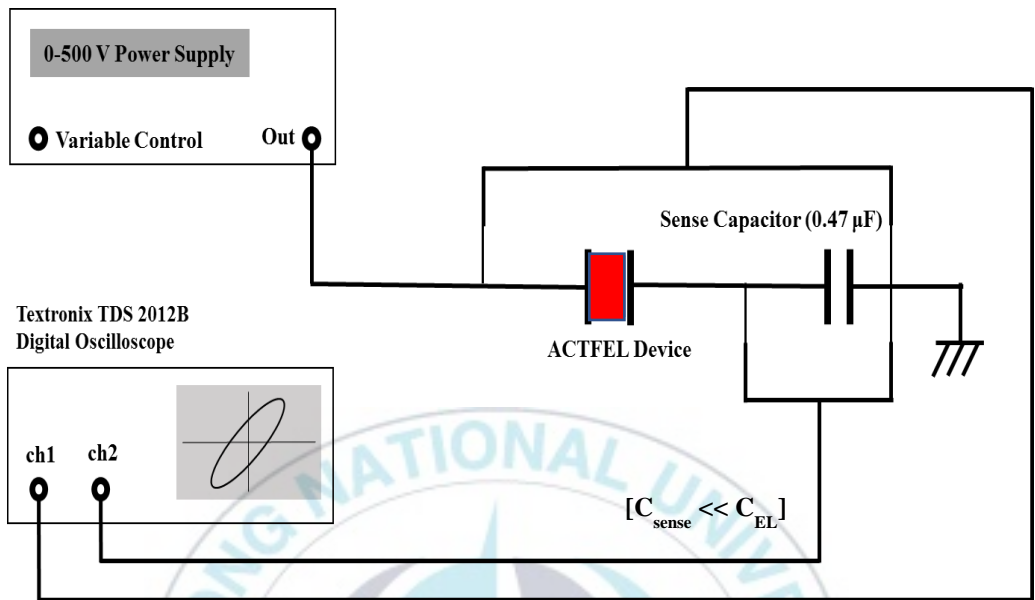


Figure 9. Sawyer-Tower Circuit Preparation

# Chapter 4

## Results and Discussion

### 1. Structural Characteristics

#### 1.1 FE-SEM Image of $\text{Y}_2\text{SiO}_5:\text{Eu}^{3+}$ phosphor

Figure 10 shows the FE-SEM image of  $\text{Y}_2\text{SiO}_5:\text{Eu}^{3+}$  ACTFEL Device deposited on silicon wafer substrate. The surface looks well uniform with minor crack around  $1\ \mu\text{m}$  size which still tolerate as an ACTFEL device. From the cross-sectional image, we can see that the thickness of phosphor is around 1,200 nm and the thickness of  $\text{SiO}_2$  dielectric layers are 400 nm each. Therefore, the total thickness of this device is approximately  $2\ \mu\text{m}$ .

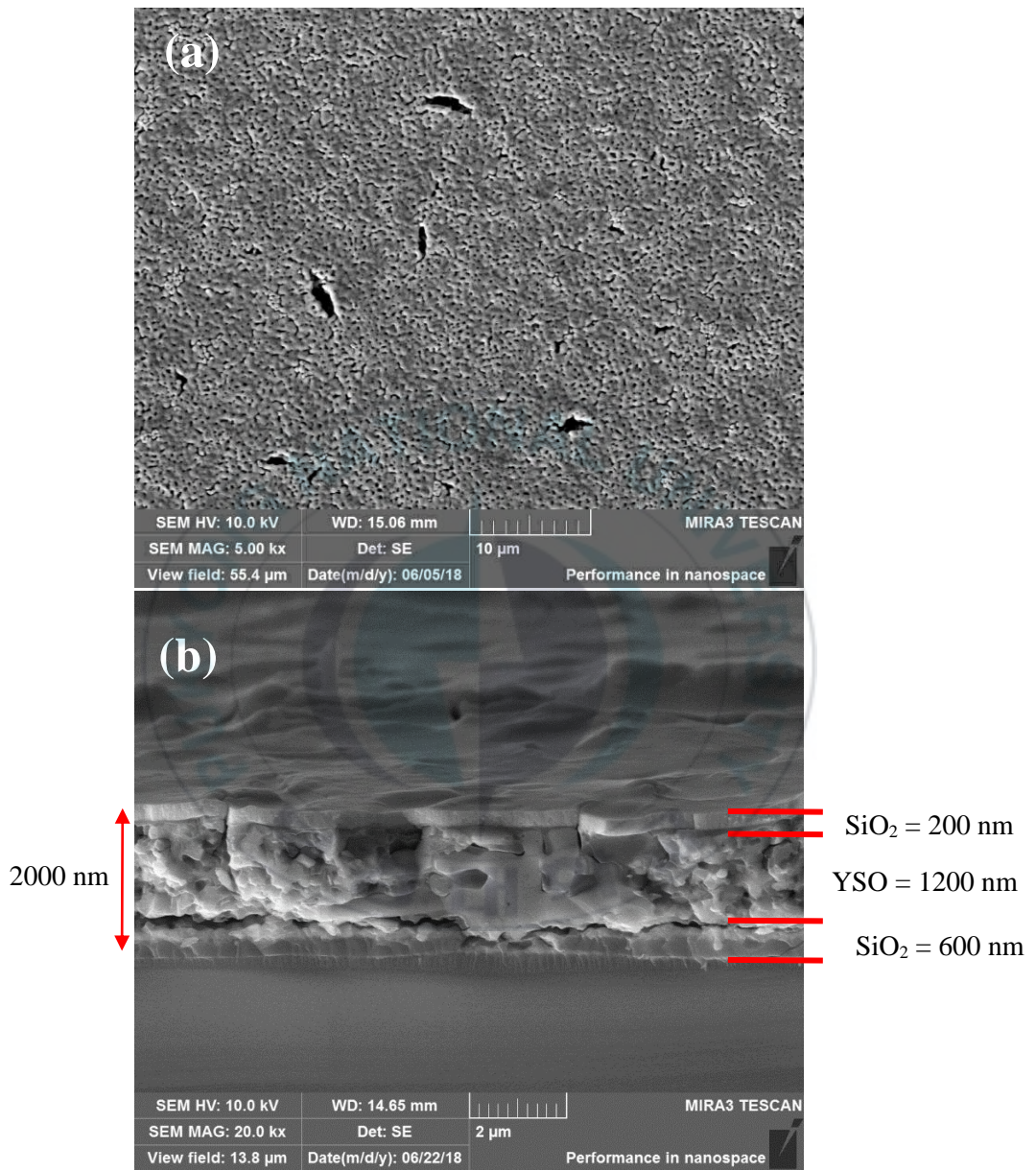


Figure 10. FE-SEM Image of  $Y_2SiO_5:Eu^{3+}$  ACTFEL Device; a) Surface Image, b) Cross-Sectional Image

## 1.2 XRD Pattern of $\text{Y}_2\text{SiO}_5:\text{Eu}^{3+}$ phosphor

Figure 11 displays the XRD pattern of  $\text{Y}_2\text{SiO}_5:\text{Eu}^{3+}$  thin film phosphor. The  $\text{Y}_2\text{SiO}_5:\text{Eu}^{3+}$  film consists of monoclinic yttrium oxide silicate (X1- $\text{Y}_2\text{SiO}_5$ , JCPDS card No. #41-0004, ★ are indicated), some  $\text{SiO}_2$  phases from  $\text{SiO}_2$  dielectric layers, and Si phase from Si wafer.

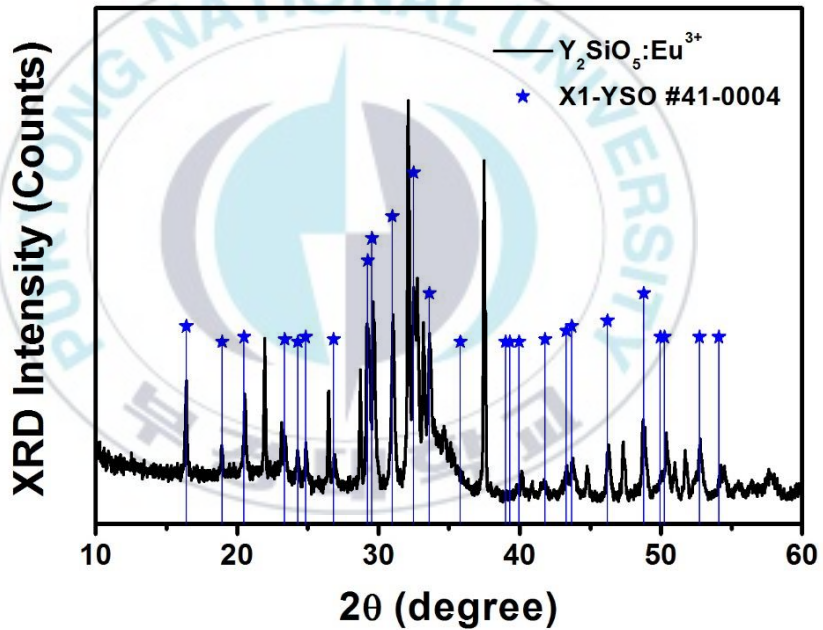


Figure 11. XRD Pattern of  $\text{Y}_2\text{SiO}_5:\text{Eu}^{3+}$  Thin Film; ★ are indicated in X1- $\text{Y}_2\text{SiO}_5$ , peaks

### 1.3 EDX Spectrum of $\text{Y}_2\text{SiO}_5:\text{Eu}^{3+}$ phosphor

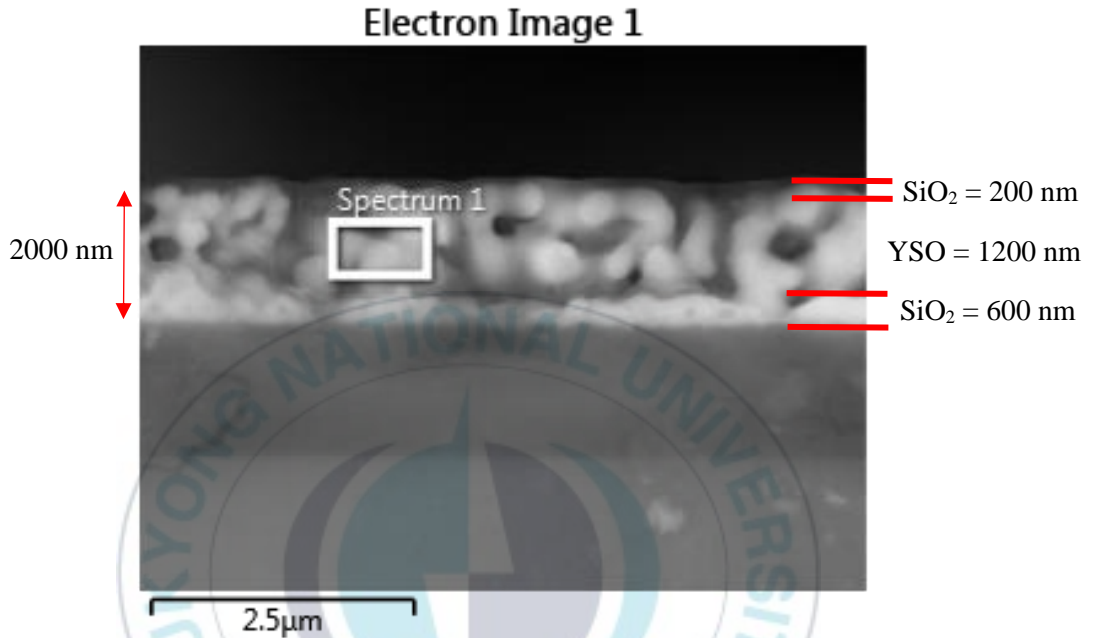


Figure 12. EDX Scan of  $\text{Y}_2\text{SiO}_5:\text{Eu}^{3+}$  Film

Figure 12 shows the EDX scan through the pores of  $\text{Y}_2\text{SiO}_5:\text{Eu}^{3+}$  film. On table 2, the scan pores contains Y, Si, O and Eu elements with several of concentrations. The finally actual doped Eu molar concentration was determined as  $0.35/21.40 = 1.63\%$ , which was similar with the initial doped concentration without any loss during fabrication process. Silicon contents of  $\text{SiO}_2$  layers and Si wafer were detected together with silicon content of pure  $\text{Y}_2\text{SiO}_5$  host, and thus, the actual stoichiometry of  $\text{Y}_2\text{SiO}_5$  final product was

overestimated to be SiO<sub>2</sub> excess as follow;  $Y_{21}Si_{41}O_x = Y_2Si_4O_x = Y_2SiO_x + 3SiO_2$ .

Table 2. The EDX Contents of Y<sub>2</sub>SiO<sub>5</sub>:Eu<sup>3+</sup> Thin Film

Element	Line Type	Apparent Concentration	k Ratio	Weight%	Atomic%
O	K series	4.35	0.01463	16.03	37.12
Si	K series	13.70	0.10858	31.18	41.13
Y	L series	13.24	0.13244	51.37	21.40
Eu	L series	0.39	0.00389	1.43	0.35
Total:				100.00	100.00

## 2. Optical Properties

### 2.1 PLE, PL and EL Spectra

Figure 13 exhibits the PL and PLE spectra of Y<sub>2</sub>SiO<sub>5</sub>:Eu<sup>3+</sup> phosphor. The PLE spectrum has broad 250 nm peak which results from charge transfer state (CTS) transition and sharp peak in 390 nm from f-f transition [30]. The PL spectrum has four peaks of 575, 585, 610, and 660 nm which are attributed to <sup>5</sup>D<sub>0</sub> → <sup>7</sup>F<sub>0</sub>, <sup>5</sup>D<sub>0</sub> → <sup>7</sup>F<sub>1</sub> (from magnetic dipole transition, which is strongly dependent on crystal symmetry), <sup>5</sup>D<sub>0</sub> → <sup>7</sup>F<sub>2</sub> (from electric dipole transition, which is less dependent on crystal symmetry), and <sup>5</sup>D<sub>0</sub> → <sup>7</sup>F<sub>3</sub> transition of Eu<sup>3+</sup> in Y<sub>2</sub>SiO<sub>5</sub>:Eu<sup>3+</sup> phosphor respectively [31]. It is noted that the 585 nm peak of the EL spectrum at 80 V and 400 Hz is lower than that of the PL spectrum. It means

the symmetry of activator is lowered during EL operation under higher electric field which penetrates through the phosphor layer [32, 33].

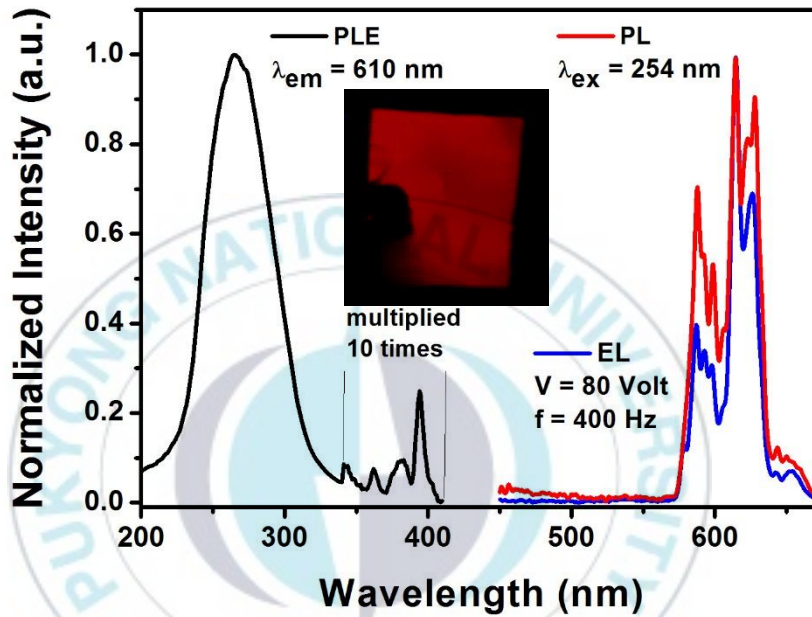


Figure 13. PLE, PL and EL Spectra of  $\text{Y}_2\text{SiO}_5:\text{Eu}^{3+}$  ACTFEL Device, inset figure: emitting condition of device

## 2.2 Decay Curve

Figure 14 depicts the decay graph of 610 nm main PL peak of  $\text{Y}_2\text{SiO}_5:\text{Eu}^{3+}$  phosphor. The well-known decay time of  $\text{Eu}^{3+}$  ion is about in millisecond order [34]. The figure 14 shows that the average single exponential PL decay curve of this phosphor with 610 and 585 nm emission and 250 nm excitation is 1.5 ms. The millisecond decay time causes to saturating the EL intensity at the critical applied frequency which is estimated to be proportionally inverse with decay time. The EL device shows the saturation behavior of the EL intensity at the critical frequency of about 600 Hz, which is confirmed in the EL intensity dependence on frequency as follows.

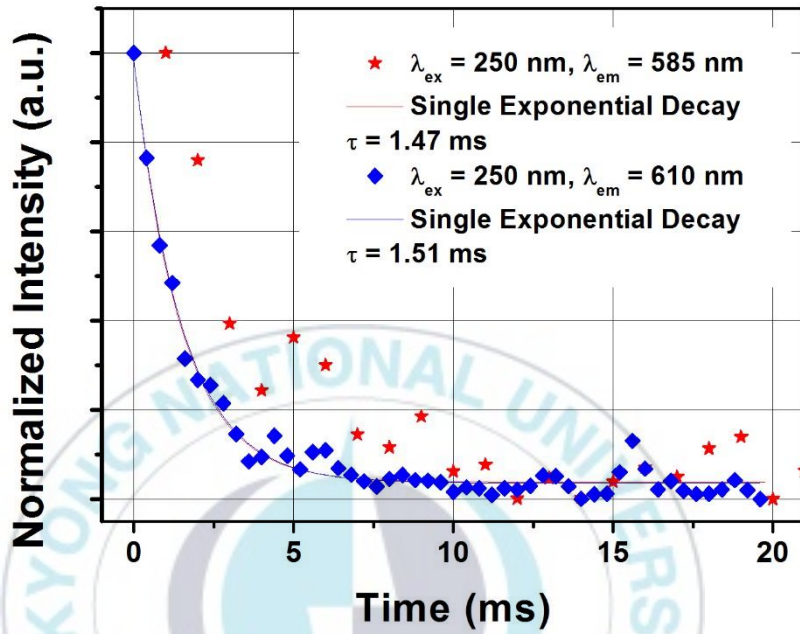


Figure 14. PL Decay Time of  $\text{Y}_2\text{SiO}_5:\text{Eu}^{3+}$  Phosphor

## 2.3 Time Chart

Figure 15 displays the EL time chart of voltage ( $V$ ), current ( $I$ ) and EL Intensity time chart in AC pulse power supply with 1 Hz of frequency. From the figure, we can see that the EL emits both in the positive state and negative state of the AC pulse power supply. The current-EL time chart has similar characteristics which proved that the EL was working when the current flows through the device. The EL time chart, which has longer tail around 100 ms, looks not similar to the PL decay time. It is due to different measuring conditions: PL decay time measured with short pulse of excitation light while EL long tail measured with continuous pulse voltage source.

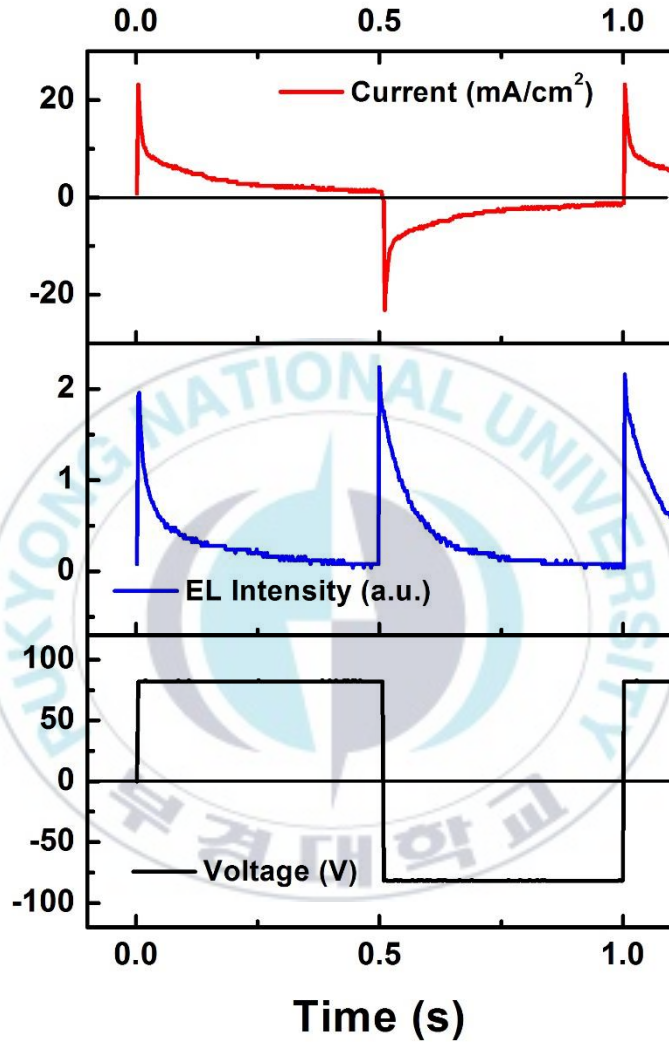


Figure 15. V-I-EL Time Chart of the ACTFEL Device

## 2.4 Reflectance spectrum

Figure 16 displays the reflectance graph of  $\text{Y}_2\text{SiO}_5:\text{Eu}^{3+}$  EL device deposited on Si wafer substrate. From the graph we can see that the reflectance simulation interface pattern of two layers  $\text{Y}_2\text{SiO}_5$  phosphor which and  $\text{SiO}_2$  dielectric has similar characteristics with the reflectance of measurements. Therefore, the thickness according to this reflectance matches the thickness provide by the FE-SEM image.

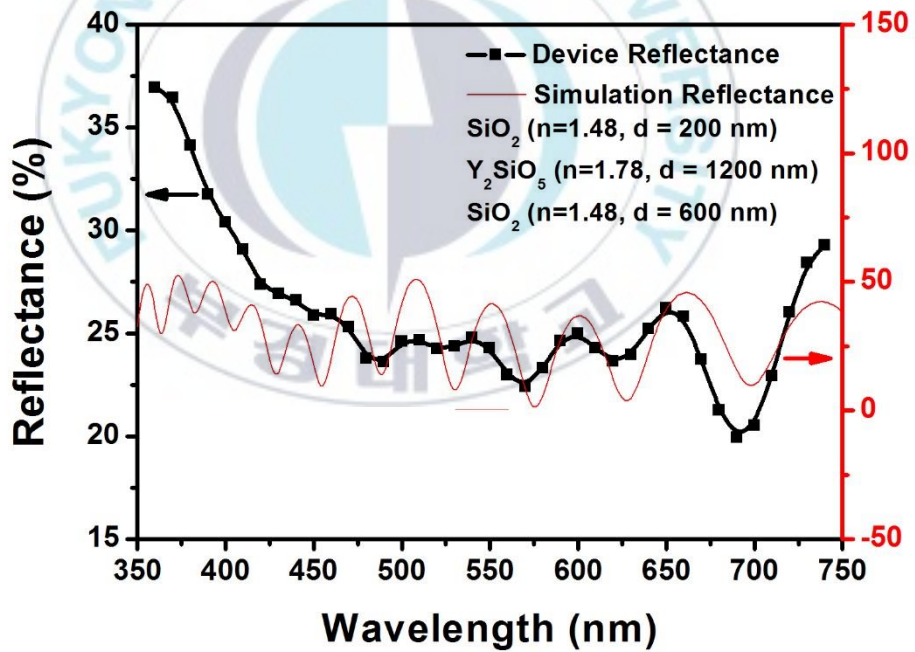


Figure 16. Reflectance of  $\text{Y}_2\text{SiO}_5:\text{Eu}^{3+}$  Thin Film on Si Wafer Substrate

The simulation reflectance was measured by Filmetrics reflectance calculator which used same calculation engine for thin film measurements system based on complex-matrix for multilayer structure of Fresnel Equations below.

$$r = \frac{n_1 \cos \theta_1 - n_2 \cos \theta_t}{n_1 \cos \theta_1 + n_2 \cos \theta_t}$$

While  $r$  is the reflection coefficient,  $n$  is the refractive index,  $\theta_i$  is angle of incidence, and  $\theta_t$  transmitted angle.

### 3. Opto-Electric Properties

#### 3.1 Voltage-Dependent EL Spectra

Figure 17 shows the Eu-activated EL spectra with various voltages from 40 to 80 V for a fixed 400 Hz frequency. The peak wavelength is 610 nm and the full width at half maximum (FWHM) is 20 nm. The CIE color coordinate is  $x = 0.6069$  and  $y = 0.344$ . The characteristics of Eu-activated EL spectra are slightly changed with increasing voltages ( $\Delta x = +0.0052$ ,  $\Delta y = -0.0043$ ), which means that the spectra are stable with a change of voltages. On the contrary, ZnS-based EL is strongly dependent on the voltage, which is blue-shifted at

higher applied voltage. It is due to the change in the energy band gap of ZnS by high electric field [35].

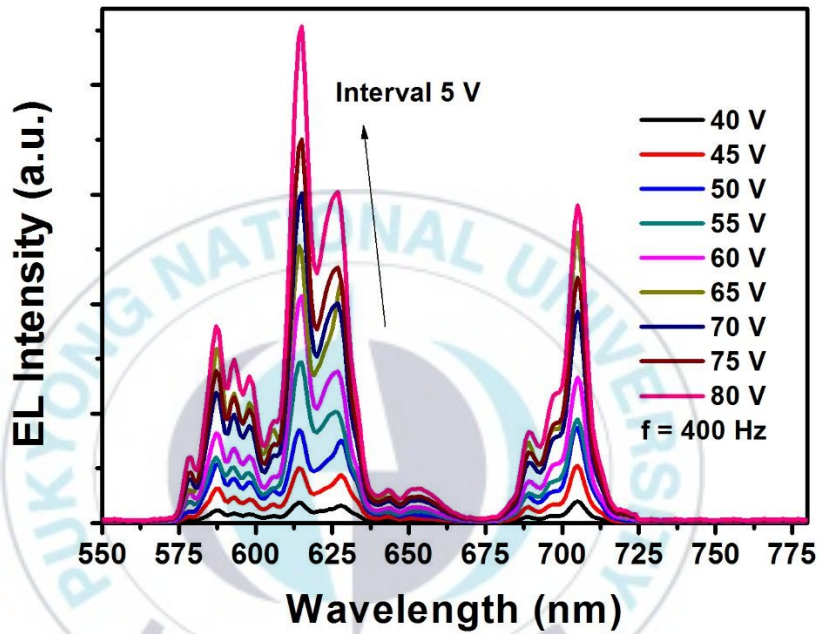


Figure 17. EL Spectra of ACTFEL Device with the Various Applied Voltage at 400 Hz

The EL device driven by alternating current (AC) sinusoidal power supply at various voltages. The threshold voltage of  $\text{Eu}^{3+}$ -activated device is 40 V, therefore the electric field (E) of the phosphor layer is calculated as  $2.0 \times 10^7$  V/cm as follows:

$$Q_1 = \frac{\epsilon_1 V_1}{d_1} = Q_2 = \frac{\epsilon_2 V_2}{d_2}$$

$$\frac{V_2}{V_1} = \frac{\epsilon_1 d_1}{d_2 \epsilon_2} \rightarrow \frac{V_2}{V_1} = \frac{3.9 \times 1200}{800 \times 3.4}$$

$$E = \frac{V_2}{d_2} = 2.0 \times 10^7 \text{ V/cm},$$

where  $\epsilon_1 = 3.9$  and  $\epsilon_2 = 3.4$  are the relative dielectric constants of  $\text{SiO}_2$  and  $\text{Y}_2\text{SiO}_5$ , respectively, and  $d_1 = 800$  nm and  $d_2 = 1200$  nm are the relative film thicknesses of  $\text{SiO}_2$  and  $\text{Y}_2\text{SiO}_5$ , respectively. The luminance of EL device is given by following equation [36].

$$L = L_0 e^{(-bV^{-\frac{1}{2}})}$$

$L_0$  and  $V_0$  are constants, which depend on the particle size of phosphor, the concentration of the activator, and the thickness of the emissive layer. The equation exhibits that the logarithm of  $L$  is directly proportional to  $V^{-1/2}$ . Luminance ( $L$ ) versus applied voltage ( $V$ ) varying from 40 to 80 V with fixed 400 Hz frequency is plotted at figure 18.

The experimental results are roughly in accordance with the above equation which exponentially increases on increasing of voltages. It suggests

that the excitation mechanism of  $\text{Eu}^{3+}$ -activated  $\text{Y}_2\text{SiO}_5$  ACTFEL phosphor is similar with that of the conventional EL. A luminance of  $1.6 \text{ cd/m}^2$  was obtained at 80 V and 400 Hz.

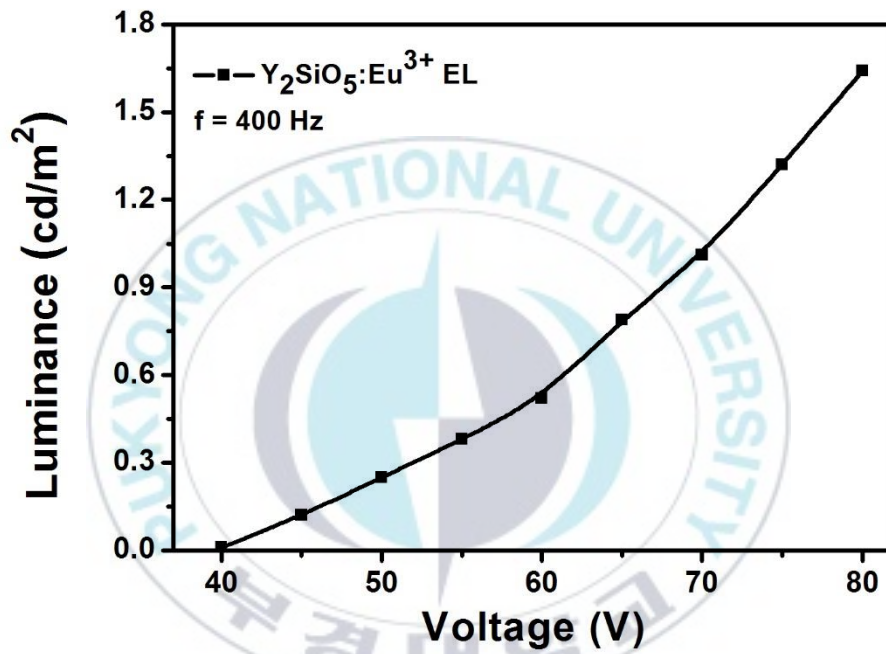


Figure 18. Luminance-Voltage ( $L$ - $V$ ) Characteristics of ACTFEL Device

### 3.2 Frequency-Dependent EL Spectra

Figure 19 displays EL spectra at the several of frequencies from 100 Hz to 1000 Hz with a fixed voltage of 80 V. The EL spectra have no effect or independent with the change of frequency. On the contrary ZnS-based EL reported the strong blue shift with increasing of frequency [37].

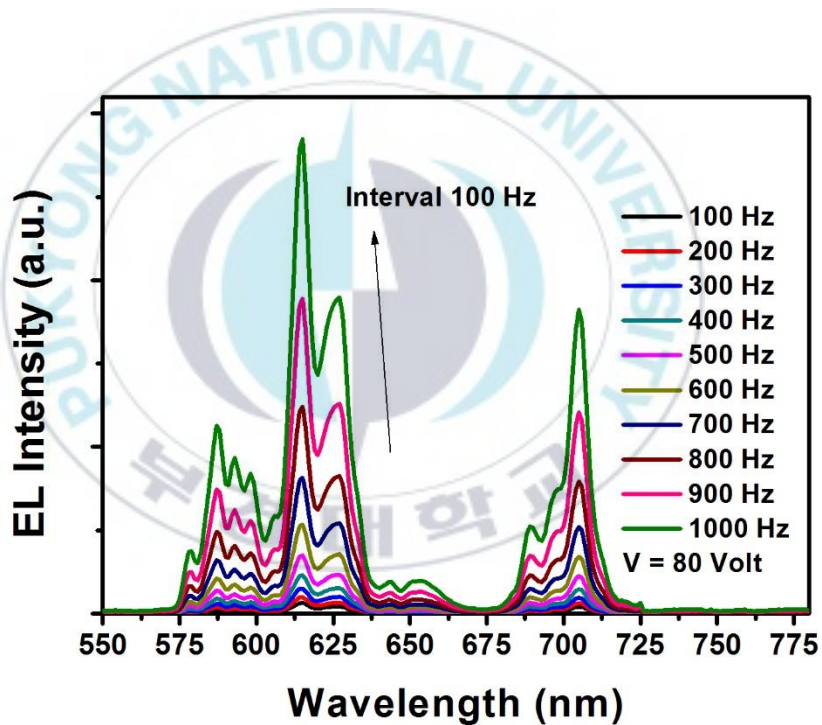


Figure 19. EL Spectra of ACTFEL Device with the Various Applied Frequencies at 80 V

The luminance of  $\text{Y}_2\text{SiO}_5:\text{Eu}^{3+}$  device is linearly increased with the increasing frequency in lower range below 600 Hz. This phenomenon can be

explain by the increasing excitation chance of the host lattice or  $\text{Eu}^{3+}$  ions with increasing of frequency. However, at the higher frequency the luminance is saturated. This saturated condition was caused by the long decay time of  $\text{Y}_2\text{SiO}_5:\text{Eu}^{3+}$  phosphor due to forbidden transition of  $\text{Eu}^{3+}$  ions. So, the EL excitation happens before the full decay of its emission. The saturation frequency ( $f_s$ ) can be calculates approximately with the inverse of decay time ( $\tau$ ):  $1/\tau = 1/1.5 \text{ ms} = f_s \approx 600 \text{ Hz}$ , which can be seen on figure 20. The EL spectra has no color change with a slight change of the CIE color coordinates in 1/1000 order of  $\Delta x = -0.0017$ ,  $\Delta y = -0.0002$ .

Furthermore, we can conclude that the  $\text{Y}_2\text{SiO}_5:\text{Eu}^{3+}$  based ACTFEL device is not spectrally influenced by both frequency and also applied voltage. This condition possesses higher stability in operating condition.

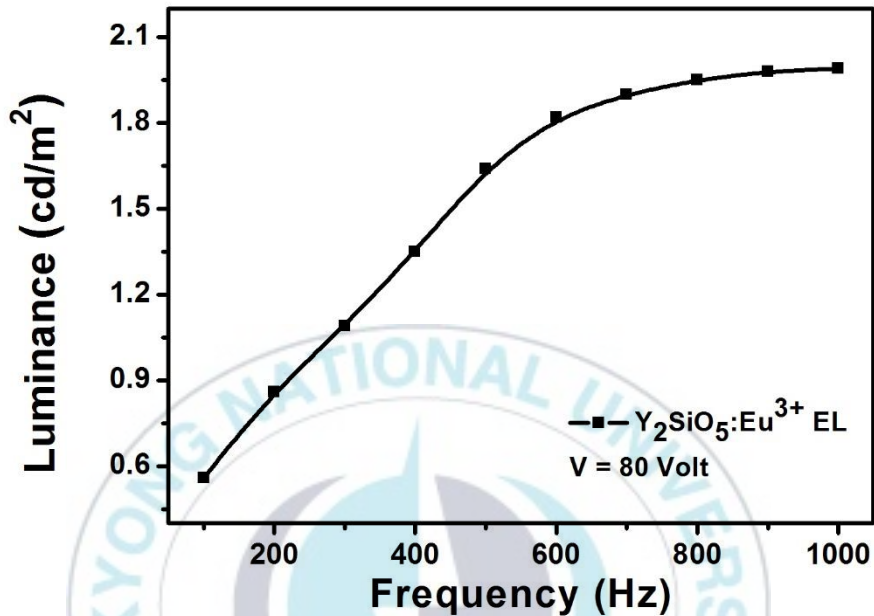


Figure 20. Luminance-Frequency ( $L$ - $f$ ) Characteristics of ACTFEL Device

### 3.3 Temperature-Dependent EL Spectra

Figure 21 depicts the EL and PL intensity with the several of temperature of ACTFEL device at fixed sinusoidal voltage of 80 V and frequency of 400 Hz. At the lower temperature between 20°C to 80°C, the EL intensity was steady and relatively stable. However, after 80°C the EL intensity was gradually decreased along with increasing of temperature and at the 150°C, the luminance remained as 40% compared with the first condition.

On the other hand, the PL behavior responses on temperature was continuously decreased. This result can be explained by the thermal quenching effect of the phosphor which reduces the amount of radiative transitions of activators at higher temperature. It is noted that the temperature dependence of EL is less severe than that of PL. It can be explained the fact that temperature dependence of EL is assisted by the injection of more electrons from trapped states between phosphor and dielectric layers due to their thermal release in addition to the internal thermal quenching effect within activators.

Finally, we can conclude that the  $\text{Eu}^{3+}$ -activated  $\text{Y}_2\text{SiO}_5$  ACTFEL device is not degraded its luminance under  $80^\circ\text{C}$  and it shows consistent spectrum which can be seen on figure 22 and the change of CIE color ( $\Delta x = -0.0008$ ,  $\Delta y = -0.0008$ ). These results mean the ACTFEL device was independent and stable to the extreme operation condition.

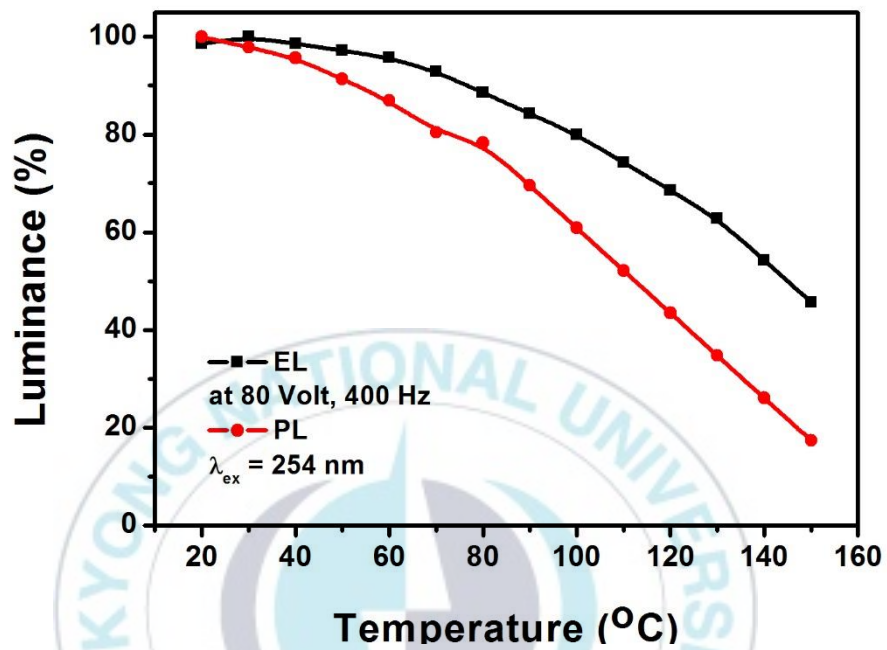


Figure 21. EL and PL-Temperature (EL, PL-T) Characteristics of ACTFEL Device

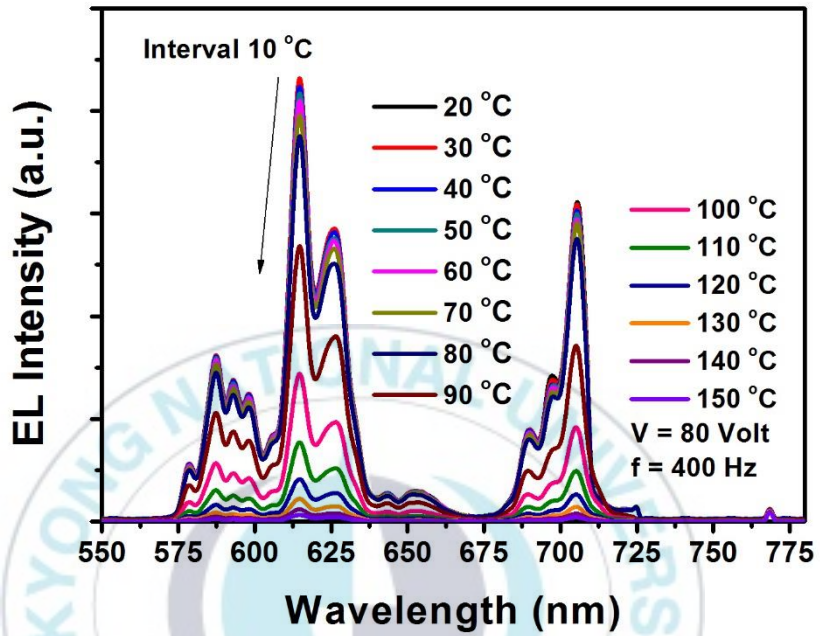


Figure 22. EL Spectra of ACTFEL Device with the Various Temperatures at 80 V and 400 Hz

## 4. Electrical Properties

### 4.1 Q-V Characteristics

Figure 23 shows the charge density ( $Q$ ) versus voltage ( $V$ ) at the sinusoidal voltages from 40 V to 80 V at fixed frequency of 400 Hz. The  $Q$ - $V$  curve is measured by conventional Sawyer-Tower circuit using 0.47  $\mu$ F sense capacitor. As the increasing of voltage, the remaining charge densities at the transient voltage of zero are increased from 1.14 nC/cm<sup>2</sup> at 40 V to 5.04 nC/cm<sup>2</sup> at 80 V. The charge density reaches maximum point of 23.4 nC/cm<sup>2</sup> at 80 V in the falling phase of applied voltage.

The integrated area of the  $Q$ - $V$  graph means the power consumption of the EL device in one cycle. The calculated full power consumption of this device is 25 mW/cm<sup>2</sup> which obtained at 80 V and 400 Hz.

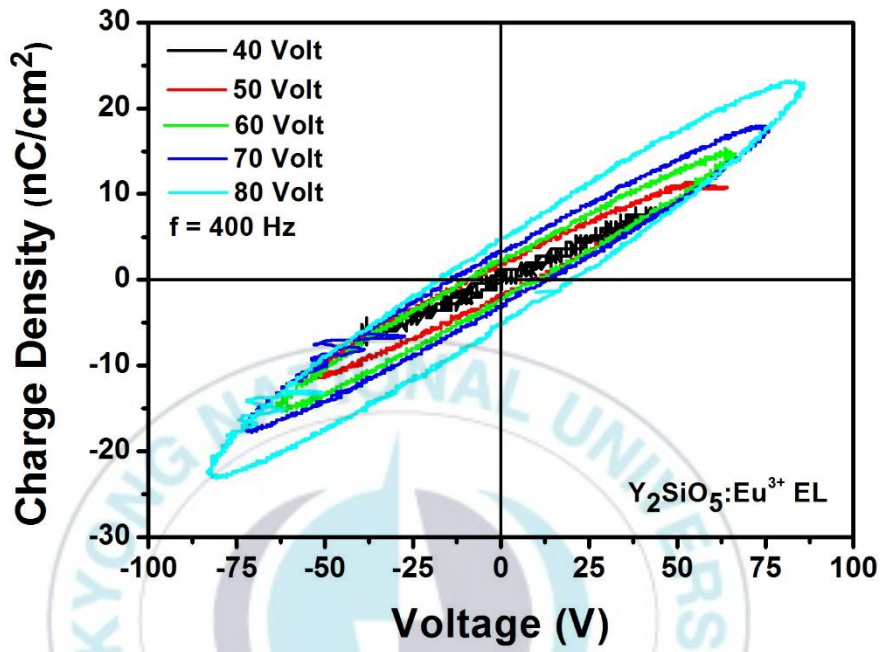


Figure 23. Charge Density-Voltage ( $Q$ - $V$ ) Characteristics of ACTFEL Device

## 4.2 Efficiency and Power Consumption

Figure 24 shows the efficiencies, luminance intensities, power consumptions and current densities with the increasing of voltages. Assuming a diffusive EL emission surface of ACTFEL device, the luminous efficiency ( $\eta$ ) can be calculated by following equation [38];

$$\eta = \frac{\pi L}{fA}$$

Where  $L$  is the luminance in the unit of  $\text{cd/m}^2$ ,  $f$  is the frequency in the unit of Hz, and  $A$  is the encompassed area of  $Q$ - $V$  diagram in the figure 20 in the unit of  $\text{W/m}^2$ . So, the maximum luminous efficiency of this device is 0.6  $\text{lm/W}$  at 45 V and 400 Hz. Furthermore, this device also has comparable luminous efficiency at its operating voltage which is 0.5  $\text{lm/W}$  on average.

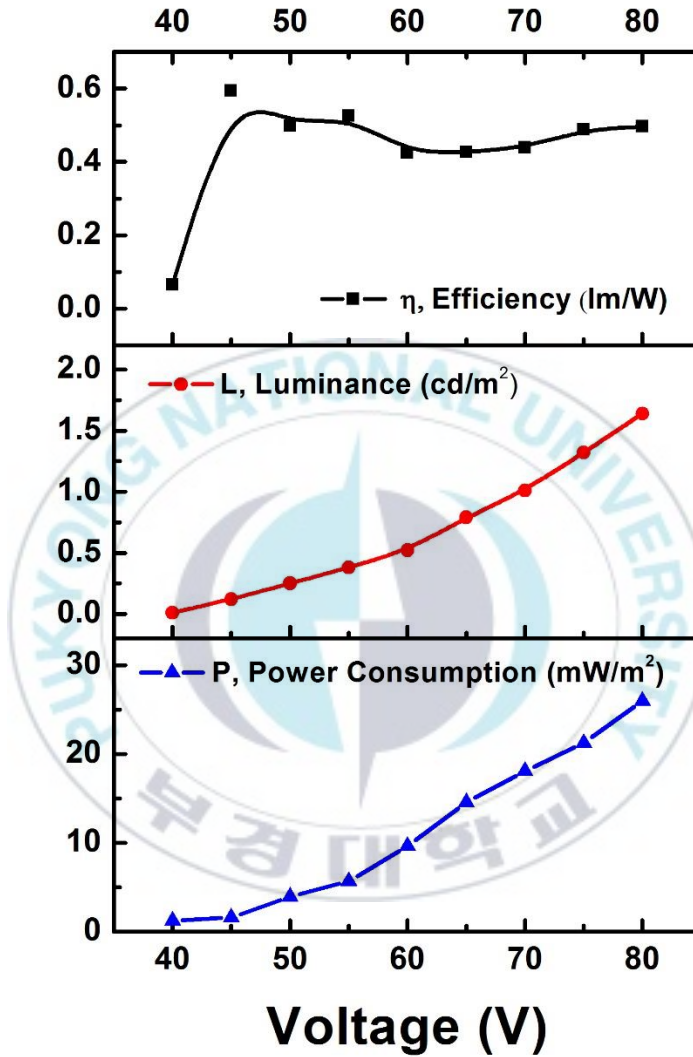


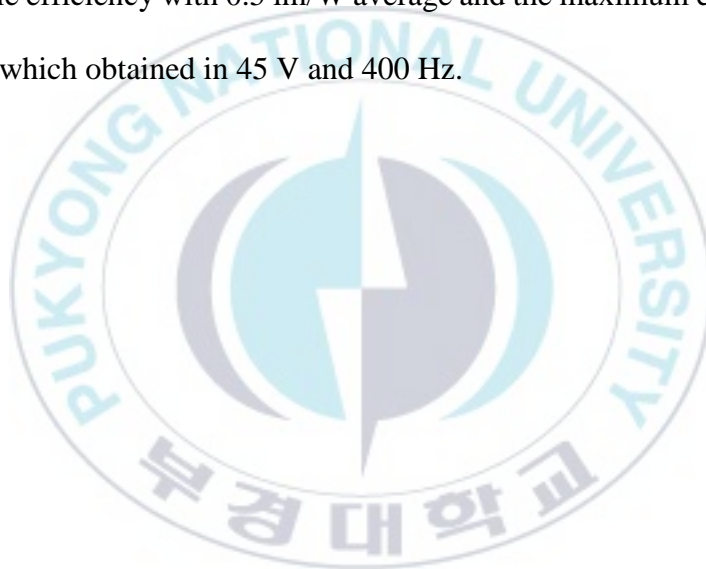
Figure 24. Efficiency, Luminance, and Power Consumption-Voltage ( $\eta, L, P-V$ )  
 Characteristics of ACTFEL Device

## Chapter 5

### Conclusion

A red alternating current thin film electroluminescent (ACTFEL) device has been demonstrated by coating the  $\text{Eu}^{3+}$ -activated  $\text{Y}_2\text{SiO}_5$  phosphor on Si wafer. This ACTFEL device consists of double  $\text{SiO}_2$  insulating layer which sandwiched the phosphor layer, and ITO sputter as the top electrode. The phosphor was coating by sol-gel spin coating method and synthesized in high temperature through solid state reaction method. The photoluminescence (PL) emission spectrum and electroluminescence (EL) spectrum has identical characteristic with 610 nm red emission peak. The device shows exponentially increase of its luminance with the increasing of voltage. The maximum luminance of  $1.6 \text{ cd/m}^2$  was obtained at 80 V and 400 Hz. On the other hand, the device luminance is linearly increased with the increasing of applied frequency and steady after it reached its saturation point. The saturation frequency of the device is around 600 Hz which obtained from inverting the decay time of its PL emission. The temperature-dependent EL

luminance shows the device luminance is stable until the temperature reach 80°C. However, the EL response is gradually decrease its luminance after 80°C due to thermal quenching effect of the phosphor which reduce the chance of recombination of  $\text{Eu}^3$  ions with the host lattice. Finally, due to its low power consumption, only 25  $\text{mW}/\text{m}^2$  on 80 V and 400 Hz, the EL shows comparable efficiency with 0.5  $\text{lm}/\text{W}$  average and the maximum efficiency is 0.6  $\text{lm}/\text{W}$  which obtained in 45 V and 400 Hz.



## References

- [1] G. Muller, Solid state luminescence theory, Materials and devices, 136, 1993.
- [2] T. Miyata, T. Minami, K. Saikai, and S. Takata, J. Lumin. 60, 926, 1994.
- [3] A. Kitai and X. Ouyang, SID Digest, 94. 572, 1994.
- [4] T. Minami, Thin-film oxide phosphors as electroluminescent materials, Mat. Res. Soc., 558, 29, 2000.
- [5] Q. Zhang, K. Pita, S. Buddhudu, and C. Kam, Luminescent properties of rare-earth ion doped yttrium silicate thin film phosphors for a full-colour display, J. Phys. D: Appl. Phys. 35, 3085, 2002.
- [6] X. Ouyang, A. Kitai, and T. Xiao, Electroluminescence of the oxide thin film phosphors  $Zn_2SiO_4$  and  $Y_2SiO_5$ , J. Appl. Phys., 79, 3229, 1996.

- [7] Y. Liu, C. Xu, H. Matsui, T. Imamura, and T. Watanabe, Preparation and luminescence of rare-earth-activated  $\text{Y}_2\text{SiO}_5$  thin films by metallorganic decomposition, *J. Lumin*, 87, 1297, 2000.
- [8] W. Yen, S. Shionoya, and H. Yamamoto, *Phosphor handbook*, CRC Press, 2007.
- [9] C. Ronda, *Luminescence from theory to applications*, Wiley-VCH, New York, 2008.
- [10] P. Bamfield, and M. Hutchings, *Chromic phenomena technological applications of color chemistry*, 2nd edn, The Royal Society of Chemistry, Cambridge, 2010.
- [11] G. Distrieu, *J. Chem. Phys.*, 22, 587, 1936.
- [12] N. Vlasenko, S. Zynio, and V. Kopytko, The effect of Mn concentration on ZnS: Mn electroluminescence decay, *PSSA*, 29, 671, 1976.
- [13] J. Hunt, M. Wisherd, and L. Bonham, Infrared absorption spectra of minerals and other inorganic compounds, *Anal. Chem.*, 22 (12), 1478, 1950.
- [14] J. Millán, and P. Godignon, Wide band gap power semiconductor devices, *Elec. Device*, 2013.

- [15] A. Fischer, Injection electroluminescence, *Sol. State Elec.*, 2 (4), 232, 1961.
- [16] S. Mishra, D. Kshatri, A. Khare, S. Tiwari, and P. Dwivedi, Fabrication, characterization and electroluminescence studies of SrS: Ce<sup>3+</sup> ACTFEL device, *Mater. Lett.*, 198, 101, 2017.
- [17] S. Lee, K. Fujita, and T. Tsutsui, Emission mechanism of double-insulating organic electroluminescence device driven at ac voltage, *Jap. J. Appl. Phys.*, 44(1), A477, 2003.
- [18] Y. Nakanishi, S. Mori, T. Nakamura, H. Tatsuoka, H. Kuwabara, and Y. Hatanaka, Effect of insulating layer structural properties for thin-film electroluminescent devices, *Mater. Chem. Phys.*, 43, 292, 1996.
- [19] Y. Abe, M. Fuyama, K. Onisawa, and Y. Ono, Effects of the cell structure on ZnS:Mn El characteristics, *Elec. and Comm.*, 72 (10), 87, 1989.
- [20] J. Ebelman, and M. Boutquet, *Ann. Chim. Phys.*, 17, 54, 1946.
- [21] B. Rao, D. Mukherjee, and B. Reddy, Novel approaches for preparation of nanoparticles, *Nanostructures*, 1, 2017.

- [22] L. Peurrung and D. Graves, Spin coating over topography, *IEEE Trans. On Semi. Manuf.*, 6(1), 72, 1993.
- [23] T. Minami, H. Toda, and T. Miyata, *J. Vac. Sci & Tech. A*, 19, 1742, 2001.
- [24] J. Gonzalez-Ortega, N. Perea, and G. Hirata, White light emission from  $\text{Y}_2\text{SiO}_5\text{:Ce}$ ,  $\text{Tb}$  films excited by electroluminescence, *Opt. Mater.*, 29, 47, 2006.
- [25] G. Blasse, and B. Grabmaier, Radiative return to the ground state: Emission, *Lumin. Mater.* 33, 1993.
- [26] C. Lin, H. Wang, D. Kong, M. Yu, X. Liu, Z. Wang, and J. Lin, Silica Supported Submicron  $\text{SiO}_2\text{@Y}_2\text{SiO}_5\text{:Eu}^{3+}$  &  $\text{SiO}_2\text{@Y}_2\text{SiO}_5\text{:Ce}^{3+}/\text{Tb}^{3+}$  Spherical Particles with a Core–Shell Structure: Sol–Gel Synthesis and Characterization, *Eur. J. Inorg. Chem.*, 3667, 2006.
- [27] Z. Liu, Y. Huang, X. Yi, B. Fu, G. Yuan, J. Wang, J. Li, and Y. Zhang, Analysis of photoluminescence thermal quenching: guidance for the design of highly effective p-type doping of nitrides, *Sci. Rep.*, 6, 32033, 2016.

- [28] S. Ponce, Y. Jia, M. Giantomassi, M. Mikami, and X. Gonze, Understanding thermal quenching of photoluminescence from first principles, *Mater. Sci.*, 2015.
- [29] S. Bouden, A. Dahi, F. Hauquier, H. Randriamahazaka, and J. Ghilane, Multifunctional indium tin oxide electrode generated by unusual surface modification, *Sci. Rep.*, 6, 36708, 2016.
- [30] Y. Liu, C. Xu, H. Matsui, T. Imamura, and T. Watanabe, Preparation and luminescence of rare-earth-activated  $Y_2SiO_5$  thin films by metallorganic decomposition, *J. Lumin.*, 87, 1297, 20000.
- [31] Q. Zhang, K. Pita, S. Buddhudu, and C. Kam, Luminescent properties of rare-earth ion doped yttrium silicate thin film phosphors for a full-colour display, *Phys. D: Appl. Phys.*, 35, 3085, 2002.
- [32] Y. Zhang, Y. Dong, J. Xu., and B. Wei,  $Ge^{4+}$ ,  $Eu^{3+}$ -codoped  $Y_2SiO_5$  as a novel red phosphor for white LED applications, *Phys. Status Solidi A*, 5, 214, 2017.
- [33] A. Patra, P. Ghosh, P. S. Chowdhury, A. R. C. Alencar, Marcio, W. B. Lozano, N. Rakov, and G. S. Maciel, *J. Phys. Chem. B*, 109, 10142, 2005.

- [34] P. Ghosh, S. Sadhu, and A. Patra, Preparation and photoluminescence properties of  $\text{Y}_2\text{SiO}_5:\text{Eu}^{3+}$  nanocrystals, *Phys. Chem. Chem. Phys.*, 8, 3342, 2006.
- [35] L. Wen, B. Liu, S. Wang, H. Zhang, W. Zhao, Z. Yang, Y. Wang, J. Su, L. Li, F. Long, Z. Zou, and Y. Gao, Enhancing light emission in flexible AC electroluminescent devices by tetrapod-like zinc oxide whiskers, *Opt. Exp.*, 24, 23419, 2016.
- [36] P. Zalm, G. Diemes, H. Klasens, *Philips Res. Rep.* 10, 205, 1955.
- [37] J. Ibanez, E. Garcia, L. Gil, M. Mollar, and B. Mari, *Displays*, 28, 112, 2007.
- [38] L. Tannas, *Flat-Panel Display and CRTs*, Van Norstrand Reinhold, Dordrecht, Netherlands, 281, 1985